Author Manuscript

Author Manuscript

Author Manuscript

Author Manuscript

HHS Public Access

Author manuscript

Int J Radiat Oncol Biol Phys. Author manuscript; available in PMC 2019 May 01.

Published in final edited form as:

Int J Radiat Oncol Biol Phys. 2018 May 01; 101(1): 88–96. doi:10.1016/j.ijrobp.2018.01.042.

Sensitization of hypoxic tumors to radiation therapy using ultrasound sensitive oxygen microbubbles

John R. Eisenbrey, PhD[1,*], **Rawan Shraim, BS**[2], **Ji-Bin Liu, MD**[1], **Jingzhi Li, MD**[1,3], **Maria Stanczak, MS**[1], **Brian Oeffinger, MS**[2], **Dennis B. Leeper, PhD**[4], **Scott W. Keith, PhD**[5], **Lauren J. Jablonowski, PhD**[1], **Flemming Forsberg, PhD**[1], **Patrick O'Kane, MD**[1], and **Margaret A. Wheatley, PhD**[2]

[1]Department of Radiology, Thomas Jefferson University, Philadelphia, PA 19107, USA

[2]School of Biomedical Engineering and Health Sciences, Drexel University, Philadelphia, PA, 19104, USA

[3]Department of Vascular Ultrasonography, Xuanwu Hospital, Capital Medical University, Beijing, China

[4]Department of Radiation Oncology, Thomas Jefferson University, Philadelphia, PA 19107, USA

[5]Division of Biostatistics, Department of Pharmacology and Experimental Therapeutics, Thomas Jefferson University, Philadelphia, PA 19107, USA

Abstract

Much of the volume of solid tumors typically exists in a chronically hypoxic microenvironment which has been shown to result in both chemo- and radiotherapy resistance. Systemic delivery of oxygen prior to therapy has proven largely ineffective in reversing this resistance. Surfactant-shelled oxygen microbubbles that can be injected intravenously and used to locally elevate tumor oxygen levels when triggered by noninvasive ultrasound have been previously reported. In this work, we show that these agents successfully and consistently increase breast tumor oxygenation levels in a murine model by 20 mmHg, significantly more than control injections of saline or untriggered oxygen microbubbles ($p < 0.001$). Using photoacoustic imaging, we also show that oxygen delivery is independent of hemoglobin transport, enabling oxygen delivery to avascular regions of the tumor. Finally, we show that overcoming hypoxia by this method immediately prior to radiation therapy nearly triples radiosensitivity. This improvement in radiosensitivity results in roughly 30 days of improved tumor control, providing statistically significant improvements in tumor growth and animal survival ($p < 0.03$). Findings from this study demonstrate the potential advantages of ultrasound-triggered oxygen delivery to solid tumors and warrant future efforts into clinical translation of the microbubble platform.

*Address correspondence to: John Eisenbrey, PhD, Thomas Jefferson University, Department of Radiology, 132 South 10th St, Philadelphia, PA 19107, John.eisenbrey@jefferson.edu.

Publisher's Disclaimer: This is a PDF file of an unedited manuscript that has been accepted for publication. As a service to our customers we are providing this early version of the manuscript. The manuscript will undergo copyediting, typesetting, and review of the resulting proof before it is published in its final citable form. Please note that during the production process errors may be discovered which could affect the content, and all legal disclaimers that apply to the journal pertain.

Author Manuscript Author Manuscript Author Manuscript Author Manuscript

Keywords

Microbubble; oxygen; tumor hypoxia; radiotherapy; ultrasound

Introduction

Breast cancer is the most prevalent form of cancer and second most widespread cause of cancer death in women (1). Within the United States, over 12% of women will develop breast cancer in their lifetime and require treatment (1). Treatments for breast cancer vary based on subtype and staging, but involve external beam radiation therapy in conjunction with surgery or chemotherapy in 52% of early stage cancers and 45% of late stage cancers (2). Additionally, radiation therapy remains a mainstay in the treatment of a variety of other solid tumors.

It has been well documented that the chaotic and uncontrolled angiogenic growth required for solid tumor formation also results in chronic tissue hypoxia due to inadequate oxygen (O_2) delivery (3). While healthy subcutaneous tissue generally exhibits O_2 partial pressures (pO_2) from 40–60 mmHg, many tumors exhibit partial pressures as low as 2 mmHg (4). Although data is limited due to difficulties of quantifying oxygenation levels in patients, the median tumor pO_2 has been reported at 10.0 mmHg in breast tumors (5). Hypoxia has been identified as a major hurdle within the treatment of breast cancer, particularly during radiation therapy (5). Initial work with hypoxia-associated radiotherapy resistance focused on cell culture under hypoxic conditions to establish radiosensitivity curves as described by Rockwell et al. (6). Cells under hypoxic conditions have been shown to be more resistant to radiation than fully oxygenated tissue, with the slope of the dose-response curve three times less steep for hypoxic than well oxygenated cells. (7). This resistance has been attributed to the need for molecular O_2 to generate free radicals during radiation exposure (8), but has also been attributed to potential hypoxia-induced genomic changes leading to increased heat shock proteins and limited apoptosis potential (9). Importantly, radiotherapy resistance is more pronounced at lower pO_2 levels (<20 mmHg), but can be overcome almost instantaneously via localized O_2 delivery (10, 11).

A variety of systemic approaches for overcoming tumor hypoxia immediately prior to therapy have been proposed including hyperbaric chambers, carbogen breathing, erythropoietin injections, and pharmacological agents such as pentoxifylline and nicotinamide to increase blood flow, but these have failed to successfully translate clinically (12–16). More recent research efforts that now target more focused approaches such as pharmacologic respiratory inhibition or oxygen scavengers entrapped within the tumor to inhibit the rate of oxygen consumption (17–19). Ultrasound-sensitive microbubbles containing oxygen ($SE61O_2$) for localized O_2 delivery prior to radiation therapy have been previously proposed by our group (20). These agents have been shown to be stable, sensitive to local ultrasound, and capable of raising the mean tumor pO2 to as much as 20 mmHg O_2 in solid tumors (20). The purpose of this study was to validate previous oxygen delivery findings in a breast tumor model, optimize delivery parameters for tumor oxygenation,

Author Manuscript Author Manuscript Author Manuscript Author Manuscript

identify mechanisms of oxygenation, and demonstrate the efficacy of tumor radiosensitization.

Materials and Methods

Cell Line and Reagents

The human triple negative breast cancer cell line MDA-MB-231 was purchased from ATTC (Manassas, VA, USA) and maintained in exponential growth in complete RMPI 1640 (Thermo Fisher Scientific, Waltham, MA). Culture medium was supplemented with 10% Fetal Bovine Serum and 1% penicillinstreptomycin (Thermo Fisher). Cell lines were cultured in a humidified 37°C incubator with 5% CO_2.

Implantation and Tumor Growth

The animal protocol was approved by the IACUC of Thomas Jefferson University following National Institute of Health guidelines for animal care and experiments. Breast cancer tumors were grown in female immunodeficient, nude mice (Charles River Labs, Malvern, PA, USA) by injecting 1×10^6 cells with 100 μL matrigel (Thermo Fisher) subcutaneously into the right hind limb. Animals were monitored for signs of pain or distress and changes in weight based on IACUC guidelines. Tumor growth was monitored twice per week using caliper measurements.

Microbubble Fabrication

Microbubbles were fabricated based on a previously reported method using lyophilized surfactant-shelled microbubbles and recharging them with a desired gas (20). Briefly, Span 60 and water soluble Vitamin E (Tocopheryl – α *Polyethylene glycol succinate) (Fisher Scientific) are autoclaved, suspended in solution and sonicated in the presence of octoflouropropane and the resultant microbubbles separated using floatation methods to create surfactant shelled microbubbles (termed SE61). Following microbubble separation, the agents are flash frozen using liquid nitrogen (N_2), then freeze dried in the presence of glucose as a lyoprotectant and capped under vacuum. As part of this study, microbubbles were then recharged with O_2 (forming $SE61O_2$) or N_2 (forming $SE61N_2$).

Oxygen Delivery Experiments

Extent and duration of changes to intratumoral pO_2 were quantified using two approaches. Using the first approach, 8 animals were inoculated based on the techniques described above and tumors grown to 5–8 mm in the largest diameter. Animals were then anesthetized using a mixture of ketamine (75 mg/kg administered subcutaneously) and acepromazine (1 mg/kg subcutaneously) and placed on a warming blanket. Under ultrasound guidance, a 21G catheter was then placed into the tumor interstitium via a percutaneous approach. A fiber optic pO_2 probe connected to an OxyLite 2000 system (Oxford Optronics, Oxford, U.K.) was then introduced through the catheter and the tip location visually confirmed by the fluorescent light at the tip of the probe. Following placement, both the probe and animal were taped to the warming blanket to minimize movement during scanning.

Author Manuscript Author Manuscript Author Manuscript Author Manuscript

All animals received the following microbubble administrations in randomized order through a 24G tail vein catheter: a 0.1 ml bolus of $SE61O_2$ followed by a 0.05 ml saline flush during ultrasound triggering at the tumor, a 0.1 ml bolus of $SE61O_2$ followed by a 0.05 ml saline flush without ultrasound triggering at the tumor or a 0.15 ml saline flush with ultrasound triggering. Partial pressures of oxygen were obtained every 5 seconds from baseline (prior to injection) until pO_2 readings returned to baseline. Acoustic triggering was performed using a Siemens S3000 scanner with 9L4 probe (Siemens Healthineers, Mountain View, CA). A flash-destruction/replenishment sequence was employed to first monitor microbubble perfusion into the tumor with lower intensity (mechanical index = 0.09) nonlinear ultrasound, followed by a higher intensity series of destructive pulses (mechanical index of 1.39) for four seconds. This process was repeated until pO_2 levels returned to baseline and no microbubbles were visible on ultrasound. Ultrasonic parameters of the destructive pulse were verified in a water bath with a 0.5 mm needle hydrophone (Precision Acoustics Ltd, Dorset, U.K.) placed at the beam focus using an x-y-z positioning system and last calibrated by The National Physics Laboratory (Middlesex, U.K.) in April 2016. Using identical imaging parameters (imaging depth of 3 cm and focal distance of 2 cm), destructive transmit parameters at the focus were found to be 4.2 MHz 1.6 μs pulses transmitted at a derated peak negative pressure of 2.5 MPa at a pulse repetition frequency of approximately 38 Hz.

In a second set of O_2 delivery experiments, an additional 3 tumor bearing animals were monitored using photoacoustic imaging on a Vevo2100 LAZR system with LZ250 probe (VisualSonics, Toronto, Canada). Photoacoustic imaging is an emerging technology that transmits light into the tissue at specified wavelength and detects thermos-elastic expansion using piezoelectric ultrasound elements (21). Its use in quantifying tissue oxygenation based on the shifting absorption spectra of hemoglobin depending on oxygenation state is well validated (22). Tumor bearing mice were prepared as described above and underwent photoacoustic imaging in the system's Oxy-Hemo quantification mode to determine baseline tissue oxygenation percentages. Animals then received a bolus injection of $SE61O_2$ with ultrasound triggering for 1 minute. The photoacoustic probe was then immediately returned to the same plane and oxygenation measurements again performed.

Therapy Experiments

For therapy experiments, 51 tumor bearing mice were randomly assigned to one of the five groups listed in Table 1, with the experimental group receiving $SE61O_2$ with ultrasound triggering and 5 Gy radiation. Tumors were grown to 5–8 mm in largest diameter before being anesthetized as described above. Animals receiving either $SE61O_2$ or $SE61N_2$ received a 0.1 ml bolus injection followed by 0.05 ml saline flush through a 24G tail vein catheter. Animals receiving ultrasound triggering received 75 seconds of flash/replenishment sequences described above with the choice of insonation time determined during O_2 delivery experiments. Animals receiving radiation were placed 50 cm from the radiation source and covered with 4 mm lead shielding exposing the hind limb (for treatment and ultrasound access) and tail (for venous access). Immediately following ultrasound triggering, animals then received 5 Gy from an Pantak XRAD 310 (Precision X-Ray, N. Branford, CT, USA) at

Author Manuscript Author Manuscript Author Manuscript Author Manuscript

a dose rate of 2.82 Gy/min, 310 KV, ¼ mm Cu + 1 mm Al added filtration. Dose rates were calibrated daily prior to treatment using a Victoreen R-Meter (Cleveland, OH, USA).

Following treatment, animals were returned to a heating blanket and monitored until fully recovered from anesthesia. Tumor response was monitored twice per week by caliper measurements by an investigator blinded to the treatment group and tumor volume quantified as:

$$Tumor\ Volume = \frac{\pi}{6} \times length \times width \times height\,. \quad (1)$$

Animals were monitored until sacrifice criteria were met, defined by IACUC guidelines as weight loss of 20 % of baseline weight, lack of any movement for prolonged periods of time, signs of self-mutilation, ulceration of the tumor or a maximum tumor dimension exceeding 20 mm.

Data Analysis

For pO_2 monitoring experiments oxygenation levels were plotted as a function of time for each group. Peak oxygenation level and time to occurrence were computed and compared between groups. For photoacoustic imaging experiments, regions of interest were drawn across the tumor and normal in plane tissue using VevoLabs software (VisualSonics) and averaged over 20 frames for each animal. Changes in tissue and tumor hemoglobin oxygenation levels after $SE61O_2$ were then computed.

For therapy experiments, tumor growth curves were calculated for each animal and normalized to tumor volume from the day of treatment. A generalized estimating equation (GEE) regression model of tumor growth over time was fitted using an identity link and assuming no intercept (i.e., zero normalized tumor growth at time zero) and first-order autoregressive correlation structure among the repeated measures on the same animal over time (23). This GEE model had time represented by a single squared regression term and was used to estimate separate growth curves for each treatment group and evaluate differences in the growth rates between groups by Wald's test with standard errors adjusted to account for the correlated repeated measurements. Ordinary least squares regression was used to estimate confidence bands for the growth curves. Survival was calculated from the day of treatment until the day each animal was sacrificed using Kaplan-Meier curves. Log rank tests were used to determine differences in survival between groups. Significance between individual group means was computed using a Student's t-test while variations between several group means was determined using a one-way analysis of variance. Statistical analysis was performed in GraphPad Prism (GraphPad Software, San Diego, CA) and SAS v9.4 (SAS Institute, Cary, NC) with significance level set *a priori* at $\alpha = 0.05$.

Author Manuscript Author Manuscript Author Manuscript Author Manuscript

Results

Microbubble Imaging

Oxygen-filled microbubbles and as a control nitrogen microbubbles ($SE61N_2$) were fabricated based on previously described methods (20). Both $SE61N_2$ and $SE61O_2$ were well tolerated in all injections. Both agents were also well visualized on nonlinear ultrasound within the tumor following injection and able to be noninvasively and locally destroyed using higher intensity destructive pulses (confirmed by the absence of visible microbubble signal immediately following a destructive pulse). An example of this perfusion and destruction sequence is provided in Figure 1 showing nonlinear $SE61O_2$ imaging mode in gold on the left and normal B-Mode imaging in grayscale on the right of the tumor immediately prior to injection (A), after microbubble perfusion into the tumor (B), during the first frame of the destructive pulse (C), during the second frame of the destructive pulse (D), immediately following the 4 seconds of higher intensity pulses (E), and approximately 2 seconds after destructive pulses during microbubble reperfusion back into the tumor (F). This sequence was continually repeated with ultrasound detection lasting 1–2 minutes.

Monitoring of Intratumoral pO_2

Averaged data from oxygen delivery experiments measured using the OxyLite system are shown in Figure 2. Animals received bolus injections of saline, $SE61O_2$ alone, and $SE61O_2$ with ultrasound triggering and no adverse events were encountered. Baseline pO_2 levels within the tumors ranged from −0.4–1.9 mmHg. No changes in pO_2 levels were detected after the injection of saline with ultrasound or $SE61O_2$ without ultrasound (largest change < 1.9 mmHg). Statistically significant levels of oxygenation were observed in tumors treated with $SE61O_2$ in combination with ultrasound ($p < 0.001$). When averaged across all animals, tumors treated with $SE61O_2$ with ultrasound demonstrated a peak increase to 19.7 ± 9.1 mmHg. Increases in pO_2 levels occurred within 15 seconds of injection and lasted at least 2 minutes in all animals with peak oxygenation achieved 75 ± 29 seconds post injection.

Photoacoustic Imaging of Tumor Oxygenation

Oxygen delivery experiments were repeated in three animals to assess changes in tumor hemoglobin levels. At baseline imaging, tumors demonstrated a percent hemoglobin oxygenation of 32.7 ± 2.7%, while the surrounding tissue yielded significantly higher hemoglobin oxygenation of 48.9 ± 6.5% ($p=0.016$). Following $SE61O_2$ delivery and ultrasound triggering, no significant differences in hemoglobin oxygenation were observed, with tumors having 32.4 ± 3.4% oxygenation ($p=0.9$), and surrounding tissue having 50.2 ± 5.0% oxygenation ($p=0.8$). An example of these photoacoustic images with quantification is provided in Figure 3.

Therapy Experiments

Data of normalized tumor growth from each treatment group is provided in Figure 4. Data were highly variable, but showed a shift towards improved tumor control with increased oxygen delivery prior to irradiation. The modeled tumor growth curves with corresponding confidence bands for each treated group are provided in Figure 5. Animals treated with

Author Manuscript Author Manuscript Author Manuscript Author Manuscript

$SE61O_2$ and ultrasound alone showed exponential growth from the time of treatment. Groups treated with radiotherapy without microbubble destruction (5 Gy radiation + ultrasound and 5 Gy radiation + $SE61O_2$) showed a slight improvement in tumor growth with a delay of approximately 3–5 days. Inclusion of microbubble cavitation without O_2 delivery (5 Gy + $SE61N_2$ + ultrasound) provided additional improvement of tumor control with tumor growth delay of roughly 6–12 days compared to the unirradiated group. Importantly, the experimental group receiving radiation, SE61O2 and ultrasound demonstrated improved tumor control with tumor growth delay of approximately 25–35 days and significantly lower growth rate versus $SE61O_2$ and ultrasound alone ($p=0.03$), 5 Gy radiation + ultrasound ($p<0.01$), 5 Gy radiation + $SE61O_2$ ($p=0.01$), and 5 Gy + $SE61N_2$ + ultrasound ($p<0.01$). No other significant differences in tumor growth rates were detected between the other groups.

Following treatment, animal survival was monitored until tumor volume and animal morbidity reached IACUC sacrifice criteria listed in the methods section. Animal survival is shown in Figure 6. No statistical differences were observed among animals receiving $SE61O_2$ and ultrasound alone, radiation without microbubble destruction (5 Gy radiation + ultrasound and 5 Gy radiation + $SE61O_2$), or microbubble cavitation without O_2 delivery (5 Gy + $SE61N_2$ + ultrasound) ($p=0.7$). However, a statistically significant improvement was observed in animals receiving $SE61O_2$ with ultrasound combined with 5 Gy radiation ($p=0.030$).

Discussion

Despite being identified as a goal for over 50 years, reversing tumor hypoxia remains an unmet clinical challenge in radiation oncology (6). The work presented here demonstrates the feasibility and potential advantages of using O_2 microbubbles to locally overcome this radiation-resistance in hypoxic tumor volumes. Previously, we reported on the synthesis and O_2 delivery potential of this formulation (20). Other groups have proposed O_2 (and other gas) delivery to solid tumors via microbubbles for radiosensitization, but intravenous delivery has been limited by microbubble stability (24–27). More recently, McEwan et al. (28) have shown impressive results using microbubble-delivered O_2 for improving sonodynamic therapy, but the role of this platform has yet to be explored in radiation therapy.

The work reported in this paper greatly expands our previous bubble development studies (20) by determining optimized radiation timing parameters, exploring the role of hemoglobin in O_2 transport, measuring tumor pO_2, and demonstrating significant improvement in tumor control. Delivery experiments presented in Figure 2 now show a consistent elevation in intratumoral pO_2 levels with a demonstrated increase to 19.7 ± 9.1 mmHg. No significant increases in pO_2 levels were observed following sonication of saline alone or injection of $SE61O_2$ without ultrasound triggering (Figure 2). While injection of $SE61N_2$ was not investigated in this study, our previous work has shown the cavitation of these microbubbles does not alter pO2 levels (20). Based on established radiosensitization curves, t20 mmHg oxygenation should nearly triple relative radiosensitivity, making tumors nearly as sensitive to radiation therapy as healthy, fully oxygenated tissue (29). While

Author Manuscript Author Manuscript Author Manuscript Author Manuscript

ultrasound triggering with this platform is focused on the tumor itself, O_2 delivery may also take place within the surrounding benign tissue. Importantly however, the asymptotic relationship between oxygenation and relative radiosensitivity shows that additional O_2 delivery to tissues with pO_2 above 40 mmHg (well below that of healthy tissue) results in only a limited increase in radiosensitivity (6, 29). Hence, while O_2 delivery using this technique may not be entirely tumor exclusive, its consequential radiosensitization is expected to be.

Photoacoustic imaging was employed to quantify tissue oxygenation changes across the heterogeneous tumor microenvironment (example images provided in Fig. 3). Interestingly, no detectable changes were observed using this quantification technique, despite invasive probe measurements proving elevated intratumoral pO_2 levels and photoacoustics demonstrating decreased oxygenation of the tumor relative to the surrounding tissue. This discrepancy is attributed to the different mechanisms of O_2 quantification. While the OxyLite system directly measures pO_2 levels using fiber-optics (30), photoacoustic quantification of oxygenation levels relies on comparing ratios of signal from oxygenated and de-oxygenated hemoglobin (22). Thus, we propose delivery of O_2 using this platform is independent of hemoglobin transport and explains the ability of molecular O_2 to penetrate into more avascular areas of the tumor. Based on evidence in the literature, microbubble cavitation may also be aiding in this delivery process. Microbubble cavitation has been shown to be a temporary, but high energy event, providing localized thermal and mechanical stimulation to the vascular endothelium (31, 32). This phenomenon has been shown to temporarily increase vascular and cellular membrane permeability, aiding in localized drug delivery (33–35). Additionally, ultrasound cavitation effects have been shown to aid in drug transport through microstreaming and acoustic radiation forces (32, 36). While we have yet to fully explore the factors behind O_2 transport with $SE61O_2$, the lack of hemoglobin dependence suggests delivery may be aided by these well documented ultrasound-induced mechanisms.

Therapy experiments performed in this work prove that significant tumor-sensitization occurs from the elevation of intratumoral pO_2 levels following ultrasound triggering of $SE61O_2$ (see Figures 5–6). Radiation therapy (5 Gy single fraction) was applied 75 seconds post microbubble injection (the time of peak oxygenation found during O_2 delivery experiments). Tumor control was highly variable as can be observed in Figure 4. Some of this variability is attributed to natural variations within *in vivo* models, but also the highly variable oxygenation data presented in Figure 2. Future work will explore mechanisms of applying more consistent and prolonged oxygenation prior to therapy. After regression modeling described above, tumors showed exponential volume growth and groups receiving radiation therapy without microbubble cavitation (5 Gy radiation with ultrasound or 5 Gy radiation with untriggered $SE61O_2$) demonstrated only slight improvements in tumor control (see tumor growth models presented in Fig. 5). Interestingly, cavitation of N_2 filled microbubbles prior to radiation therapy also demonstrated improved (albeit modest) tumor control. This phenomenon has been well described in the literature (37–41) and attributed to temporary vascular disruption from microbubble-cavitation and radiation-induced ceramide signaling in endothelial cell death (39). Improved tumoral control by inducing cavitation of our nitrogen bubbles confirms these bioeffects, although potential improvement using

Author Manuscript Author Manuscript Author Manuscript Author Manuscript

bubble-cavitation could likely be further improved with optimized treatment parameters based on the extent of radiosensitization reported in the literature (37).

Importantly, O_2 delivery via the SE61O_2 microbubble locally ruptured by ultrasound within the tumor successfully sensitized the tumors to radiation, resulting in improved tumoral control, (Fig. 5) and survival (Fig. 6). Based on data presented in Figure 5, tumor control was improved over 2X when delivering O_2 prior to radiation therapy compared to N_2 microbubble cavitation (tumor quadrupling times of 68 and 31 days respectively). Similarly, an improvement in median animal survival from 46 days with SE61N_2 to 76 days with SE61O_2 was observed (Figure 6). This level of improvement fits well with theoretical and *in vitro* radiosensitivity curves, which predict approximately 3X improved radiosensitivity when delivering 20 mmHg of O_2 to tumors with basal pO2 levels of less than 1.9 mmHg (6, 29). These results demonstrate the potential therapeutic gains available through localized O_2 delivery and sonication prior to radiation therapy.

While results from this study are encouraging, several limitations exist. Conclusions from subcutaneous human cell line xenografts in nude animals may be limited and findings should be repeated in syngeneic or orthotopic models to better replicate the tumor microenvironment in patients. Animals were sacrificed based on ethical guidelines for humane handling, and thus survival curves are somewhat artificial. Work to date using this platform has focused exclusively on breast cancer, but we expect sensitization is also likely to be beneficial in a wide variety of solid tumors with documented hypoxia (4). Oxygenation and tumor response data were highly variable (Figures 4–5). Future work will investigate larger sample sizes and better standardizing pre-radiation oxygenation. Quantification of oxygenation was performed using single point measurements in often very heterogeneous tumors and methods of O_2 imaging not employing hemoglobin absorbance should be investigated to better model O_2 kinetics following delivery. Additionally, while O_2 transport using this platform has been shown to be independent of hemoglobin, partially explaining the delivery to less vascular areas of tumors, the full mechanism of this delivery is not fully understood and should be investigated in the future. Finally, while the duration of oxygenation (< 3 min in most cases) is sufficient for this small animal model, longer oxygenation may be needed for clinical translation and methods for extending these effects should be investigated.

Conclusions

The work presented here demonstrates successful and consistent tumor oxygenation via localized microbubble O_2 delivery and substantial improvements in tumoral control, thereby warranting future investigations into the development of this microbubble delivery platform to carry O_2 or other substances for tumor radiosensitization.

Acknowledgments

This grant was support by National Institute of Health R21 CA 190926; and an equipment grant from Siemens Healthcare, Mount View, CA.

Author Manuscript Author Manuscript Author Manuscript Author Manuscript

Abbreviations

O_2	Oxygen
pO_2	Partial Pressure of Oxygen
$SE61N_2$	Surfactant-shelled microbubble with nitrogen core
$SE61O_2$	Surfactant-shelled microbubble with oxygen core

References

1. Siegel RL, Miller KD, Jemal A. Cancer Statistics, 2016. CA Cancer J Clin. 2017; 67:7–30. [PubMed: 28055103]
2. American Cancer Society. Cancer treatment and survivorship facts and figures 2012–2013. Atlanta: American Cancer Society; 2012.
3. Carmeliet P, Jain RK. Principles and mechanisms of vessel normalization for cancer and other angiogenic diseases. Nat Rev Drug Discov. 2011; 10:417–27. [PubMed: 21629292]
4. Brown JM, Wilson WR. Exploiting tumor hypoxia in cancer treatment. Nat Rev Cancer. 2004; 4:437–47. [PubMed: 15170446]
5. Vaupel P, Briest S, Hockel M. Hypoxia in breast cancer: pathogenesis, characterization and biological/therapeutic implications. Wien Wed Wochenschr. 2002; 152:334–42.
6. Rockwell S, Dobrucki IT, Kim EY, et al. Hypoxia and radiation therapy: past history, ongoing research, and future promise. Curr Col Med. 2009; 9:442–58.
7. Gray LH, Conger AD, Ebert M, Hornsey S, Scott OC. The concentration of oxygen dissolved in tissues at the time of irradiation as a factor in radiotherapy. Br J Radiol. 1953; 26:638–48. [PubMed: 13106296]
8. Hockel M, Vaupel P. Tumor hypoxia: definitions and current clinical, biologic, and molecular aspects. J Natl Cancer Inst. 2001; 93(4):266–76. [PubMed: 11181773]
9. Zhivotovsky B, Joseph B, Orrenius S. Tumor radiosensitivity and apoptosis. Exp Cell Res. 1999; 248:10–7. [PubMed: 10094808]
10. Brown JM. Tumor hypoxia in cancer therapy. Methods in enzymology. 2007; 435:297–321. [PubMed: 17998060]
11. Hodgkiss RJ, Roberts IJ, Watts ME, Woodcock M. Rapid-mixing studies of radiosensitivity with thiol-depleted mammalian cells. Int J Radiot Biol Relat Stud Phys Chem Med. 1987; 52:735–44.
12. Bernier J, Denekamp J, Rojas A, et al. ARCON: an accelerated radiotherapy with carbogen and nicotinamide in non small cell lung cancer: a phase I/II study by the EORTC. Radiother Oncol. 1999; 52:149–56. [PubMed: 10577700]
13. Kaanders JH, Bussink J, van der Kogel AJ. Review ARCON: a novel biology-based approach in radiotherapy. Lancet Oncol. 2002; 3:728–37. [PubMed: 12473514]
14. Hoskin PJ, Rojas AM, Phillips H, Saunders MI. Acute and late morbidity in the treatment of advanced bladder carcinoma with accelerated radiotherapy, carbogen, and nicotinamide. Cancer. 2005; 103:2287–97. [PubMed: 15834926]
15. Janssens GO, Rademakers SE, Terhaard CH, et al. Accelerated radiotherapy with carbogen and nicotinamide for laryngeal cancer: results of a phase III randomized trial. J Clin Oncol. 2012; 30:1777–83. [PubMed: 22508814]
16. Stone HB, Minchinton AI, Lemmon M, Menke D, Brown JM. Pharmacological modification of tumor blood flow: lack of correlation between alteration of mean arterial blood pressure and changes in tumor perfusion. Int J Radiat Oncol Biol Phys. 1992; 22:79–86. [PubMed: 1530755]
17. Burd R, Lavorgna SN, Daskalakis C, Wachsberger PR, Wahl ML, Biaglow JE, Stevens CW, Leeper DB. Tumor oxygenation and acidification are increased in melanoma xenografts after exposure to hyperglycemia and meta-iodo-benzylguanidine. Radiat Res. 2003; 159:328–35. [PubMed: 12600235]

Author Manuscript Author Manuscript Author Manuscript Author Manuscript

18. Nath K, Guo L, Nancolas B, et al. Mechanism of antineoplastic activity of lonidamine. Biochimica et Biophysica Acta. 2016:151–162.
19. Unger EC, Lickliter JD, Ruben J, et al. A phase Ib/II clinical trial of a novel oxygen therapeutic in chemoradiation of glioblastoma. Journal of Clinical Oncology. 2017; 35(15_suppl):2561–2561.
20. Eisenbrey JR, Albala L, Kramer MR, et al. Development of an ultrasound sensitive oxygen carrier for oxygen delivery to hypoxic tissue. Int J Pharm. 2015; 478:361–367. [PubMed: 25448552]
21. Beard P. Biomedical photoacoustic imaging. Interface Focus. 2011; 1:602–31. [PubMed: 22866233]
22. Needles A, Heinmiller A, Sun J, et al. Development and initial application of a fully integrated photoacoustic micro-ultrasound system. IEEE Trans Ultrason Ferroelectr Freq Control. 2013; 60:888–97. [PubMed: 23661123]
23. Zerger SL, Liang KY, Albert PS. Models for longitudinal data: a generalized estimating equation approach. Biometrics. 1988; 44:1049–60. [PubMed: 3233245]
24. Swanson EJ, Mohan V, Heir J, Borden MA. Phospholipid-stabilized microbubble foam for injectable oxygen delivery. Langmuir. 2010; 26:15726–9. [PubMed: 20873807]
25. Kawn JJ, Kaya M, Borden MA, Dayton PA. Theranostic oxygen delivery using ultrasound and microbubbles. Theranostics. 2012; 2:1174–84. [PubMed: 23382774]
26. Klegerman ME, Wassler M, Huang SL, et al. Liposomal modular complexes for simultaneous targeted delivery of bioactive gases and therapeutics. J Control Release. 2010; 142:326–31. [PubMed: 19903503]
27. Tong J, Ding J, Shen X, et al. Mesenchymal stem cell transplantation enhancement in myocardial infarction rat model under ultrasound combined with nitric oxide microbubbles. PLoS One. 2013; 8:e80186. [PubMed: 24244646]
28. McEwan C, Kamila S, Owen J, et al. Combined sonodynamic and antimetabolite therapy for the improved treatment of pancreatic cancer using oxygen loaded microbubbles as a delivery vehicle. Biomaterials. 2016; 80:20–32. [PubMed: 26702983]
29. Rockwell, S. Manual de Radiotherapia Oncologia. Yale University; New Haven CT: 1989. Principios de radiobiologia
30. Griffiths JR, Robinson SP. The OxyLite: a fibre-optic oxygen sensor. Br J Radiol. 1999; 72(859): 627–30. [PubMed: 10624317]
31. Ferrara K, Pollard R, Borden M. Ultrasound microbubble contrast agents: fundamentals and application to gene and drug delivery. Annu Rev Biomed Eng. 2007; 9:415–447. [PubMed: 17651012]
32. Leighton, T. The Acoustic Bubble. Academic Press Inc; London, United Kingdom: 1994.
33. Price RJ, Skyba DM, Kaul S, Skalak TC. Delivery of colloidal particles and red blood cells to tissue through microvessel ruptures created by targeted microbubble destruction with ultrasound. Circulation. 1998; 98:1264–1267. [PubMed: 9751673]
34. Kotopoulis S, Dimcevski G, Gilja OH, et al. Treatment of human pancreatic cancer using combined ultrasound, microbubbles, and gemcitabine: a clinical case study. Med Phys. 2013; 40:072902. [PubMed: 23822453]
35. Kooiman K, Emmer M, Foppen-Harteveld M, et al. Increasing the endothelial layer permeability through ultrasound-activated microbubbles. IEEE Trans Biomed Eng. 2010; 57(1):29–32. [PubMed: 19709954]
36. Wood AK, Sehgal CM. A review of low-intensity ultrasound for cancer therapy. Ultrasound Med Biol. 2015; 41(4):905–28. [PubMed: 25728459]
37. Czarnota GJ, Karshafian R, Burns PN, et al. Tumor radiation response enhancement by acoustical stimulation of the vasculature. Proc Natl Acad Sci USA. 2012; 109:E2033–41. [PubMed: 22778441]
38. Tran WT, Iradji S, Sofroni E, et al. Microbubble and ultrasound radioenhancement of bladder cancer. Br J Cancer. 2012; 107:469–76. [PubMed: 22790798]
39. Kim HC, Al-Mahrouki A, Gorjizadeh A, et al. Quantitative ultrasound characterization of tumor cell death: ultrasound-stimulated microbubbles for radiation enhancement. PLoS One. 2014; 9:102343.

Author Manuscript Author Manuscript Author Manuscript Author Manuscript

40. Daecher A, Stanczak M, Liu JB, et al. Localized microbubble cavitation-based antivascular therapy for improving HCC treatment response to radiotherapy. Cancer Letters. In Press.

41. Al-Mahrouki AA, Iradji S, Tyan TT, Czarnota GJ. Cellular characterization of ultrasound stimulated microbubble radiation enhancement in a prostate cancer xenograft model. Dis Model Mech. 2014; 7:363–7. [PubMed: 24487407]

Author Manuscript Author Manuscript Author Manuscript Author Manuscript

Summary

Ultrasound-sensitive oxygen microbubbles have been fabricated and shown to elevated partial oxygen pressures > 20 mmHg. The process of oxygen delivery has been shown to be independent of hemoglobin transport in the hypoxic tissue. Oxygen delivery prior to radiation therapy has also been shown to roughly triple radiosensitivity, improving tumor control and survival in an animal model for greater than 30 days.

Author Manuscript Author Manuscript Author Manuscript Author Manuscript

- No patient photos included in this manuscript.
- Conflict of interests are discussed in the COI forms attached with this manuscript
- No copyrighted material is included in this submission

Author Manuscript Author Manuscript Author Manuscript Author Manuscript

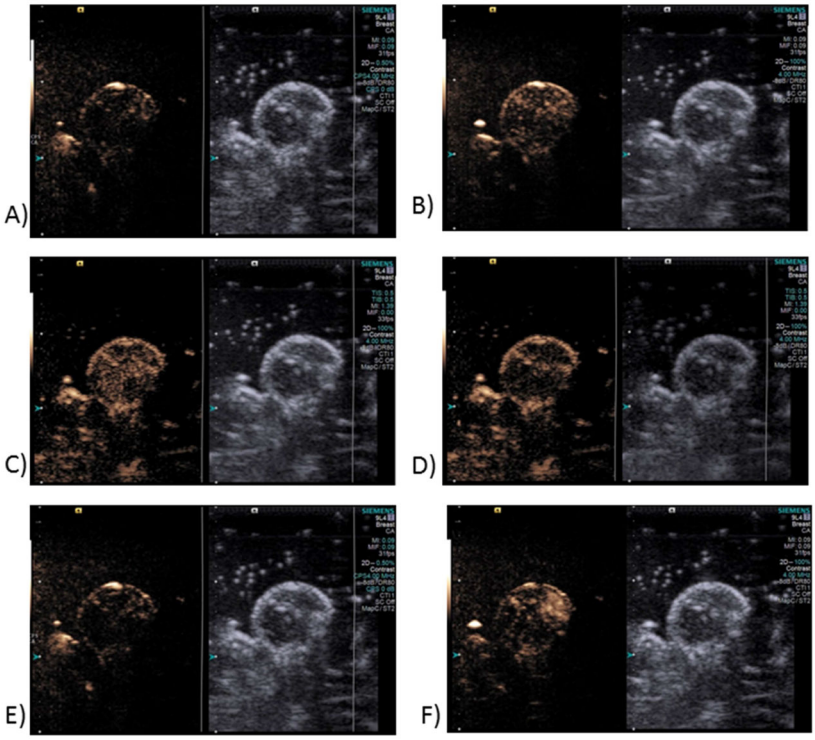

Figure 1.

Example of ultrasound sequence of dual-imaging approach showing nonlinear microbubble ($SE61O_2$) signal in gold on the left and normal B-Mode imaging in grayscale on the right of the spherical tumor immediately prior to injection (A), after microbubble perfusion into the tumor (B), during the first frame of the destructive pulse (C), during the second frame of the destructive pulse (D), immediately following the 4 seconds of higher intensity pulses (E), and approximately 2 seconds after destructive pulses during microbubble reperfusion back into the tumor (F).

Author Manuscript Author Manuscript Author Manuscript Author Manuscript

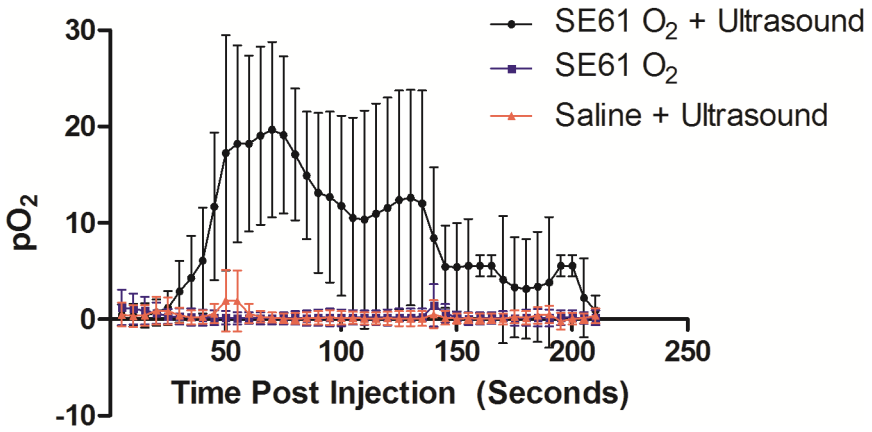

Figure 2.

Average oxygenation profiles measured by invasive OxyLite pO_2 probe demonstrating a sustained elevation of intratumoral pO_2 levels when $SE61O_2$ is insonated with ultrasound (black circles), but minimal change with the insonation of saline alone (red triangles) or injection of $SE61O_2$ without ultrasound triggering (blue squares). Data points represent mean values and error bars calculated as standard deviations.

Author Manuscript Author Manuscript Author Manuscript Author Manuscript

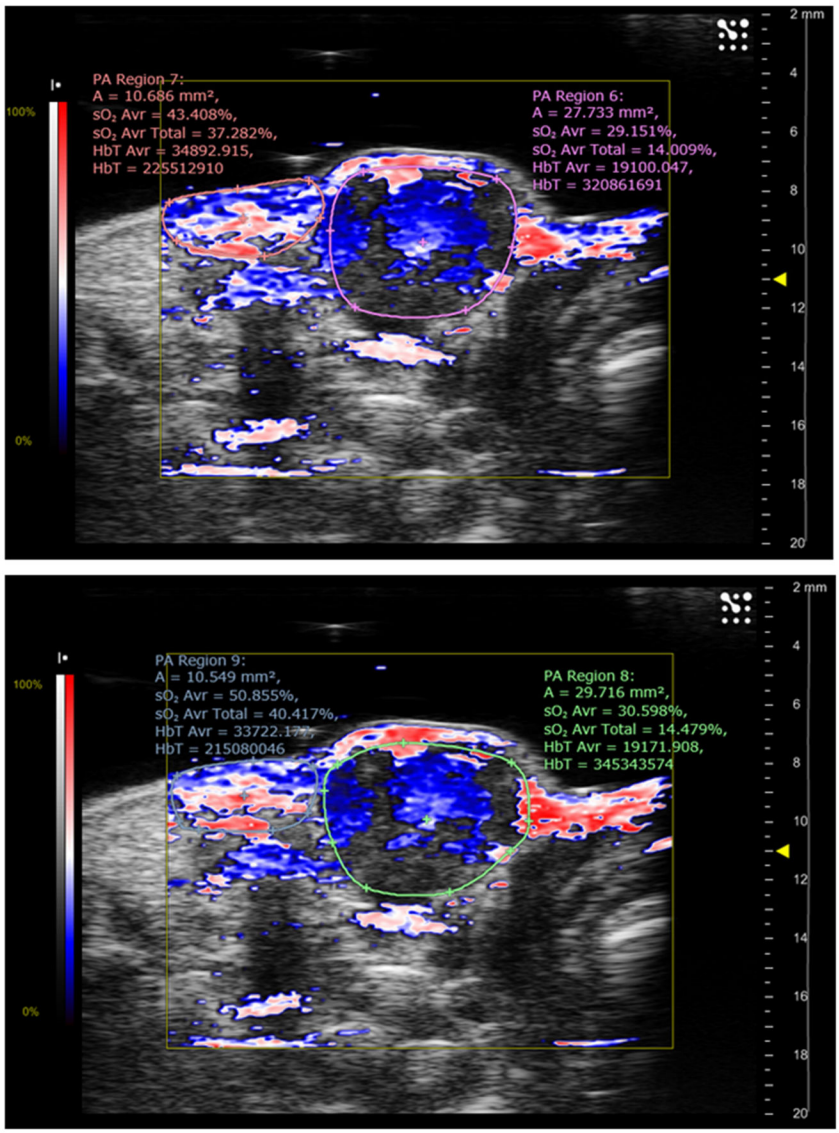

Figure 3.

Example of photoacoustic images combining B-mode ultrasound (in grayscale) with photoacoustic signal (blue to red color overlay). Prior to injection and microbubble triggering (top image), tumors showed reduced percent hemoglobin oxygenation relative to the surrounding tissue. No significant changes in hemoglobin oxygenation were observed following $SE61O_2$ injection and triggering (bottom image).

Author Manuscript Author Manuscript Author Manuscript Author Manuscript

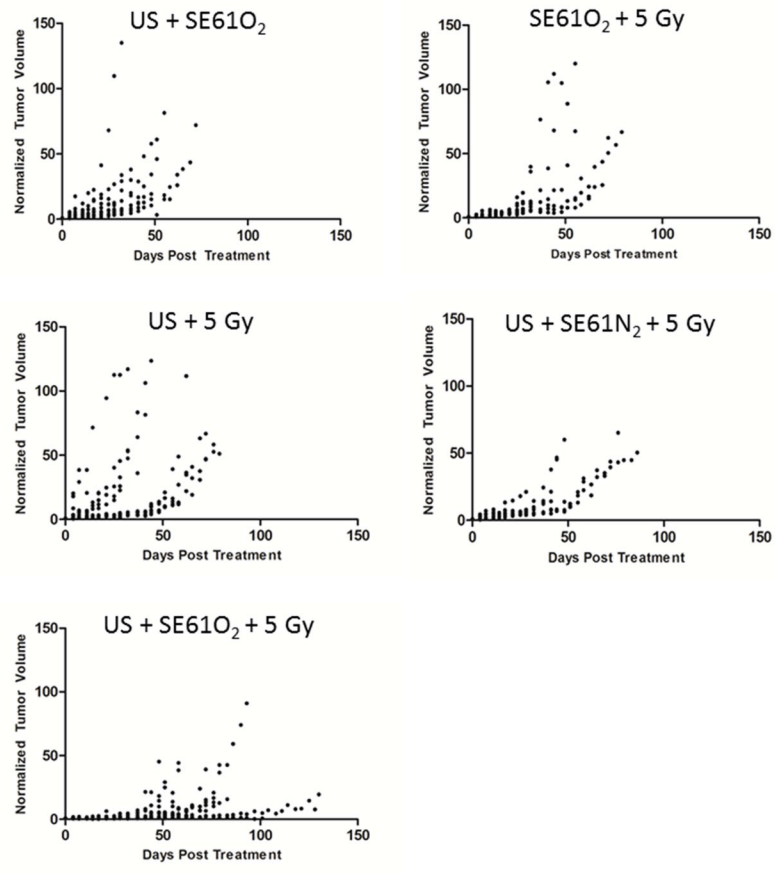

Figure 4.

Raw data showing normalized tumor growth over time. Tumor volumes were normalized to day of treatment and used to create regression model curves shown in Figure 5.

Author Manuscript Author Manuscript Author Manuscript Author Manuscript

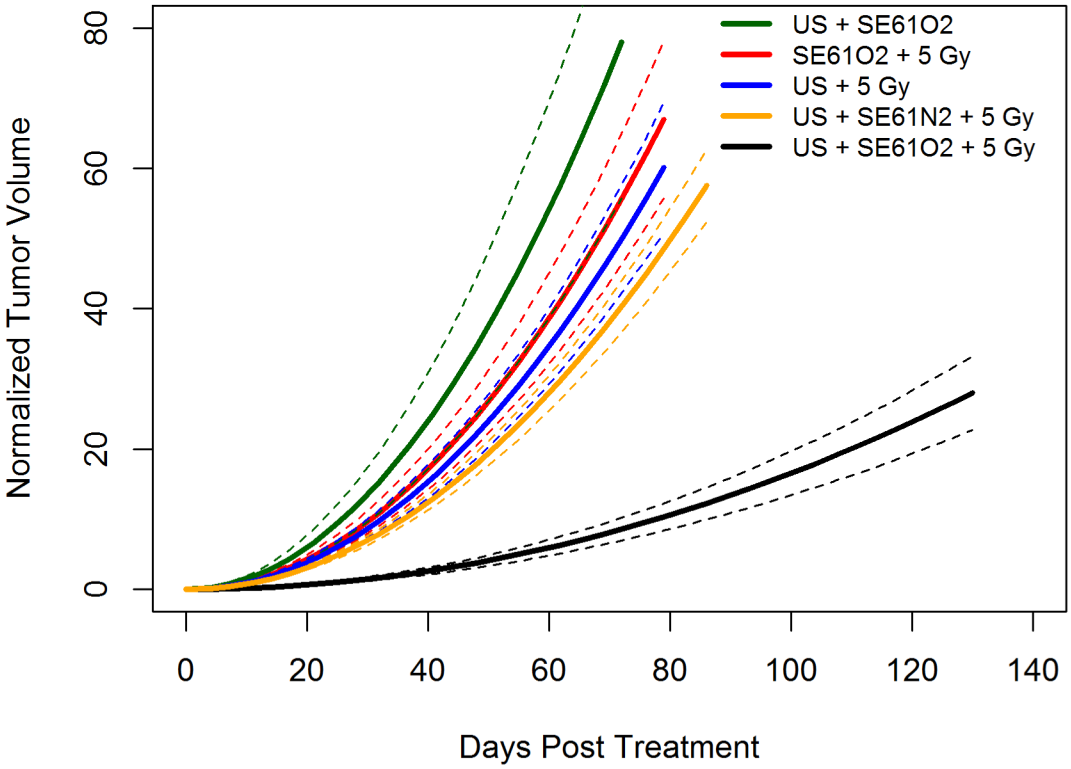

Figure 5.

Regression modeled curves of tumoral response to therapy with 95% confidence bands (dashed lines) showing the influence of ultrasound (US), SE61 bubble, and radiation. Tumor volumes were normalized to day of treatment. Green plot = US + $SE61O_2$; red plot = $SE61O_2$ + 5 Gy; blue plot = US + 5 Gy; orange plot = US + $SE61N_2$ + 5 Gy; black plot = US + $SE61O_2$ + 5 Gy.

Author Manuscript Author Manuscript Author Manuscript Author Manuscript

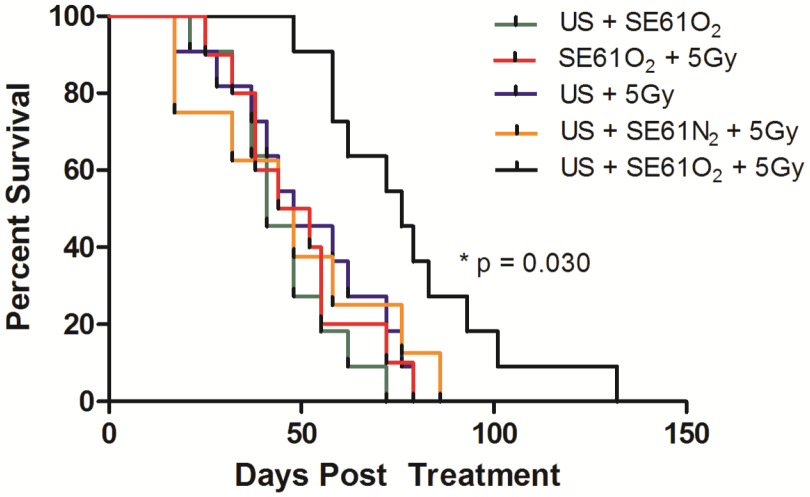

Figure 6.

Animal survival in days following treatment. Green plot = US + $SE61O_2$; red plot = $SE61O_2$ + 5 Gy; blue plot = US + 5 Gy; orange plot = US + $SE61N_2$ + 5 Gy; black plot = US + $SE61O_2$ + 5 Gy.

Author Manuscript Author Manuscript Author Manuscript Author Manuscript

Table 1

Experimental Design of In Vivo Study

Group	Radiation Therapy	Microbubble	Ultrasound	N
1	5 Gy	Oxygen	Yes	11
2	5 Gy	Oxygen	No	10
3	0 Gy	Oxygen	Yes	11
4	5 Gy	Nitrogen	Yes	8
5	5 Gy	None	Yes	11